J. Fluid Mech. (1988), *vol.* 191, *pp.* 389–418
Printed in Great Britain

Manipulation of turbulent boundary layers by outer-layer devices: skin-friction and flow-visualization results

By A. M. SAVILL† AND J. C. MUMFORD†

Fluid Dynamics Section, Cavendish Laboratory, University of Cambridge, Madingley Road, Cambridge CB3 0HE, UK

(Received 21 November 1985 and in revised form 3 November 1987)

Parametric studies have been made of devices introduced into the outer region of a low-Reynolds-number turbulent boundary layer ($Re_\theta = 1000$–3500) with a view to understanding the manner in which such 'manipulators' reduce the surface drag. The devices considered were single flat plates, a cylinder with the same drag as one of these, and two plates stacked, staggered, and in tandem, with chord Reynolds numbers Re_c in the range 1000–100000. Direct measurements of local skin friction using a floating-plate drag balance are reported together with the results of laser-sheet smoke flow visualization. The skin-friction results are in good agreement with other floating-element data while the visual and photographic studies in both stationary and convected frames completely support the hairpin description of the boundary-layer structure, and reveal that the wake of the device may play a more important role than has previously been suggested. A picture is presented of the interaction of the devices and their wakes with the hairpin eddy structure which could explain the magnitudes and shapes of the skin-friction distributions observed downstream; their dependence on the height, thickness, and if appropriate, length and spacing of the device(s); the optimum values for these parameters; and the existence of a preferred, tandem plate configuration. The results suggest that such plates do not act primarily as large-eddy break-up systems (LEBUs). Instead several 'active' mechanisms are identified which supplement the 'passive' effect of the imposed momentum defect. The suppression of large-scale motions is one of these, but, at least for our relatively thick devices, it would appear that it is an interaction between the vortices, introduced into the layer via the wake, and the near-wall structure that provides the principal mechanism for reducing the skin friction. The observation that the maximum skin-friction reduction always occurred close to the position where these vortices reached the sublayer provides strong evidence for such a view.

On this basis it is concluded that the optimum height of the device will vary inversely with Reynolds number; that the apparent optimum tandem plate spacing, s, is probably related to an interaction between their two wakes in which case the gap, g, from the trailing edge of the first to the leading edge of the second is a more appropriate parameter; and that the length of an individual plate should be greater than the height of the boundary layer to obtain the largest integrated skin-friction reduction. Comparison with other experiments indicates remarkably little change in the shape and magnitude of the C_f distributions as the plate thickness is reduced

† Present address: Engineering Department, University of Cambridge, Trumpington Street, Cambridge CB2 1PZ, UK.

Research	Manipulators studied	Re_θ	Maximum range of parameters d/δ	l/δ	h/δ	s/δ	t (mm)	Type of measurements: Drag	Flow vis.
Hefner *et al.* (1979)	1, 2, 3, plates stacked vertically	1000 → 2500	40	~ 0.8	1 → 2	—	0.8	Floating plate (1400 cm²)	—
Corke *et al* (1979)	2, 4, plates stacked vertically	900 → 4100	25 or 70*	0.94	0.8 0.43 0.21 0.09	—	0.7	Momentum balance	Smoke-wire*
Hefner *et al.* (1979)	1, 2, 3 plates stacked, staggered	1000 → 2500	50	0.56	1.10 0.58 0.24	—	0.13	Momentum balance	—
Sandborn (1981)	1, 2 in tandem	~ 4000	25	0.8	0.8 0.4	1.6 3.2	0.1	Surface hot-wire gauges	—
	Cylinder: $D/\delta = 0.02, 0.03, 0.05$; $h/\delta = 0.31, 0.01, 0.06$								
Hefner *et al.* (1983)	1, 2, 3, stacked, staggered and tandem Wire: $D/\delta = 0.01$; $h/\delta = 0.3$	1000 → 3600	80	0.1 → 2.0	0.1 → 1.2	2.5 → 15	0.254 0.127 0.025	Floating plate (2550 cm²)	Smoke-wire
Bertelrud *et al.* (1982)	2 in tandem	3000 → 7000	80	0.5 1.5	0.5 0.75	1 → 5	1.0 0.15 0.05	Preston tube	—
Corke *et al.* (1982)	1, 2, 4, stacked	2000 → 5500	55	0.8 1.2	0.7 or 1.0 0.4 or 0.5 0.2 or 0.6 0.1 or 0.2 0.6	—	0.7	Momentum balance	Smoke-wire
	and 2 in tandem			0.8	→ 0	6 → 8	0.2		

Corke *et al.* (1982)	2 in tandem	2300	60	~ 1	~ 0.5	8	0.25	Momentum balance	—
Hefner *et al.* (1983)	2 in tandem	2000 $\rightarrow 2300$	130	0.8	0.8	6.4	0.254	Momentum balance	Smoke-wire
Mumford & Savill (1984)	Single plates	1000 $\rightarrow 3500$	60	0.15 $\rightarrow 4.9$	0.1 $\rightarrow 1.25$	—	1.2 0.56	Floating plate (177 cm^2)	
	Cylinder: $D/\delta = 0.05 \rightarrow 0.07$; $h/\delta = 0.1 \rightarrow 1.25$								
And present results	Single plates and 2 in tandem	700 $\rightarrow 1600$	75	0.3 $\rightarrow 4.8$	0.1 $\rightarrow 1.25$	0.5 $\rightarrow 10$	3.2 1.2		Laser sheet + White light: stationary and convected views
	2 stacked, staggered			2.4	$\begin{Bmatrix} 1.0 \\ 0.6 \end{Bmatrix}$ or $\begin{Bmatrix} 0.6 \\ 0.3 \end{Bmatrix}$	—	3.2		
	Cylinder: $D/\delta = 0.07$; $h/\delta = 0.1 \rightarrow 1.25$								
Takagi (1983*a*)	2 in tandem	3000	56	1.4 0.7	0.8	6.6	0.1 0.05	Preston tube Clauser fit	—
Takagi (1983*b*)	Single plates	2500	47	1.6 0.8	0.8	—	0.1	Preston tube	—
	Cylinders: $D/\delta = 0.04$ or 0.08 $h/\delta = 0.8$								

TABLE 1. Range of parameters covered by previous studies and the present experiments

from 1.2 to 0.1 mm so it is likely that the same mechanisms act when the devices are of sufficiently low drag to produce a net drag reduction, and make similar contributions to the overall skin-friction reduction.

1. Introduction

Over the past two decades it has become clear that turbulent flows contain groups of coherent flow patterns, eddies superimposed on a background of essentially random fluctuations. Furthermore it appears that these eddies contain virtually all the turbulence energy and so make the dominant contributions to other quantities of interest. The emergence of such a structural picture has opened up the possibility of controlling the turbulence, perhaps to increase mixing and heat transfer or to reduce skin friction and noise, by:

(i) Selectively destroying, amplifying or reorientating one or more of the existing groups of eddies,
(ii) changing their degree of organisation, and
(iii) introducing new structures into the flow.

In the boundary layer the eddies are linked in a regenerative cycle of motions which includes both the 'bursting' and entrainment processes, and a similar cycle may exist in free-shear flows (Savill 1979). If one could interrupt this feedback loop or even merely reduce its efficiency it should be possible to reduce turbulence production, mixing and hence skin-friction drag. This might be achieved by either restricting the burst events near the wall or suppressing the entraining eddies in the outer layer. Both approaches have been investigated by several independent research groups, but early studies concentrated on large eddy break-up schemes (LEBUs) because the relaxation distances for inner-layer changes were expected to be considerably smaller.

Much of the early work was performed at the Illinois Institute of Technology under the direction of H. M. Nagib. Initial studies involved the use of screens, grids and honeycombs to control free-stream turbulence (Loerke & Nagib 1972). Similar 'management' techniques were first applied to a boundary layer by Yajnik & Acharya (1977) at the National Aerospace Laboratory, Bangalore. However, although the average skin-friction coefficient downstream of their screens and honeycombs was reduced by up to 50% the device drag of these obstacles introduced into the flow was equivalent to a 500% increase in C_f over the same distance. Accordingly, Corke, Guezennec & Nagib (1979) suggested using honeycomb-like flat plate devices with fewer horizontal members because these could provide a full range of eddy suppression and generation mechanisms, with the minimum obstruction to the flow, whilst allowing considerable latitude in matching the 'manipulator' to the dominant turbulence scales. Their experiments led to similar studies at NASA Langley by Hefner, Weinstein & Bushnell (1979). Both produced average skin-friction reductions of about 20%, but still the device drag, representing a C_f increase of 50–90%, was impractically high. Subsequent studies thus concentrated on testing a wider range of simpler constructions in an attempt to minimize the device drag while retaining sufficient integrated skin-friction reduction to obtain a net benefit (see table 1). This approach rapidly led to the configuration of two plates mounted one behind the other in tandem and indicated an apparent 'optimum' geometry: $h/\delta \approx 0.8$, $l/\delta \approx 1.0$, $t \approx 0.1$ mm and $s/\delta \approx 5$–10 (Sandborn 1981; Bertelrud, Truong & Avellan 1982; Corke, Nagib & Guezennec 1982; Hefner, Anders & Bushnell 1983) (see figure 1 for definition of parameters). Using such tandem plates net drag

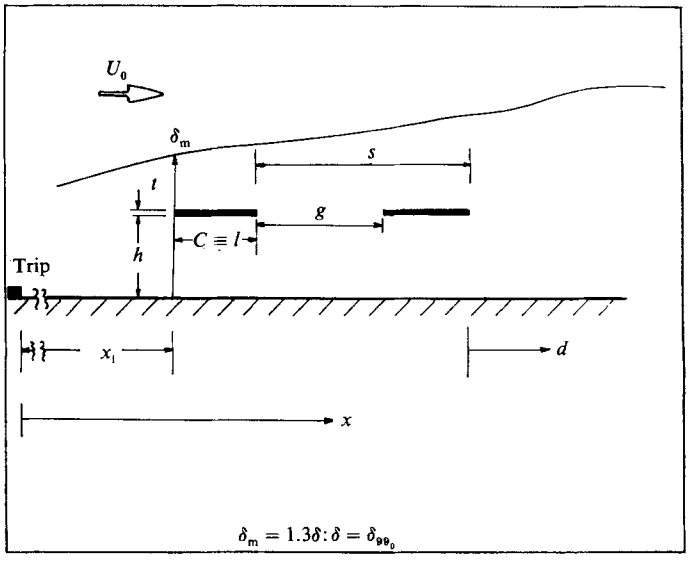

FIGURE 1. Configurational parameters for manipulator plates; subscript m denotes measurement at the leading edge of the (first) device, subscript 0 measurement at the same x-location in the undisturbed flow.

reductions ranging from between 4 and 6% over a distance of 80δ–100δ downstream of the device (Bertelrud *et al.* 1982, Hefner *et al.* 1983), up to an estimated 20% gain within only 55δ (Corke *et al.* 1982), have been reported.

A limitation of these studies was that all the net drag measurements, and indeed most of those for the skin friction alone, were based on data obtained by the so-called indirect methods, either momentum balance or wall similarity techniques. The former is potentially inaccurate and is sensitive to the weak pressure gradients and residual three-dimensionality that exist in nominally two-dimensional, zero-pressure-gradient test sections. The latter depend on the existence of a universal law of the wall, but the indication from such indirect measurements of u_τ was that the constants A and B which describe the logarithmic profile differed from their accepted values of 5.62 and 5.24 in such flows at least in the region close behind the device (see also Truong, Bertelrud & Veuve 1984; Takagi 1983*a*, *b*) and it has been shown by Acharya & Escudier (1983); Poll & Watson (1984) that this could lead to large errors. Prior to the present study only Hefner *et al.* 1983 had previously undertaken a comprehensive parametric survey and made direct drag balance measurements of C_f, but these were integrated over a large surface area. Flow visualization had been restricted to smoke-wire studies.

The present investigation combined laser-sheet and white-light-beam smoke flow visualization with hot-wire data, and localized floating-plate drag balance measurements of skin friction in an attempt to see how a single plate alters the eddy structure of the boundary layer and how these changes affect the wall region in order to understand the mechanisms whereby the skin friction is reduced. We have also studied how the degree of the reduction depends on the length, height and thickness of the plate. For comparison similar measurements have been made with a cylinder and with twin plates, stacked, staggered, and in tandem. The main aim was to try to explain the optimum device parameters in terms of the response of the eddy structure to such manipulation so we chose to use plates sufficiently thick that they

could be supported horizontally without the need for tensioning and the consequent problems of vibration. Though such devices are found not to produce net drag reductions we believe that the results are relevant to the application of thinner plates because the basic device/eddy structure interaction is unlikely to be altered by changes in the thickness of the plates and so the same mechanisms should act in all cases although their relative importance may vary.

2. Apparatus and experimental techniques

The drag measurements, skin-friction and device drag, were made in a centrifugal blower tunnel of the type described by Bradshaw (1972). Devices were mounted in the tripped roof boundary layer of the $2 \times 0.45 \times 0.47$ m Perspex-sided working section and comparative skin-friction data obtained using a floating-plate balance mounted at the end of the section (see figures 2 and 3). This incorporated a circular dural plate, 150 mm in diameter and 3 mm thick, suspended by three parallel copper wires 0.1 mm diameter and 300 mm long, so that its lower face was flush with the roof. The edge of the plate had a radial clearance of 0.5 mm, and was bevelled on the upper face. A streamwise deflection of the plate caused a variation in the light incident on a phototransistor. The output signal from this and its first derivative were amplified and fed into a solenoid which applied restoring and damping forces to a permanent magnet attached to the plate. Additional damping was provided by two oil-filled dash pots. The mean streamwise force on the plate was obtained by averaging the current in the solenoid, and for the maximum force exerted in the experiments (about 0.5 gm) the gain of the feedback circuit was sufficient to reduce the mean streamwise plate deflection to approximately 0.003 mm. The balance was calibrated against known masses suspended from a wire which was attached to the plate, and passed over a pulley. Apart from the possible systematic errors to which balances of this type may be susceptible as discussed by Winter (1977), the accuracy of the instrument was limited by temperature drift in the phototransistor. The dominant cause of the temperature fluctuations was variation of the wind speed in the tunnel, so that the errors incurred had a considerably smaller effect on the reproducibility of the results than on their absolute accuracy. Consequently, while the drift under the least favourable conditions (lowest tunnel speed) produced an error of approximately 3%, the repeatability of the measurements which determined the accuracy of the fractional drag reductions was better than 1%. Spanwise variations of mean and turbulence quantities within the boundary layer were 3% across the central 20 cm of the working section.

Initially a total of 6 flat, rectangular section dural plates: $\frac{1}{4}$, $\frac{1}{2}$, 1, 2, 3 and 5 in. by 46 cm span were tested. These were sufficiently thick (1.2 mm, and later 0.56 mm) that they could be supported under their own weight by a single threaded rod at either end. These adjustable supports could be screwed through the roof at discrete intervals thus varying the streamwise separation, d, between the manipulator and the fixed balance. The 6 stations used covered a range of d from δ to 56δ, the latter being the limit of the current experiments because the boundary-layer growth was not linear for smaller values of x_i. The drag on the plates was measured at various heights in the boundary layer on the floor of the tunnel by suspending them by four parallel wires and measuring the streamwise deflection using a cathetometer. Errors caused by the drag on the suspension wires and by spanwise non-uniformity, arising both from end effects on the plates and from the tunnel side-wall boundary layers, were minimized by repeating the measurements for a range of plates of different

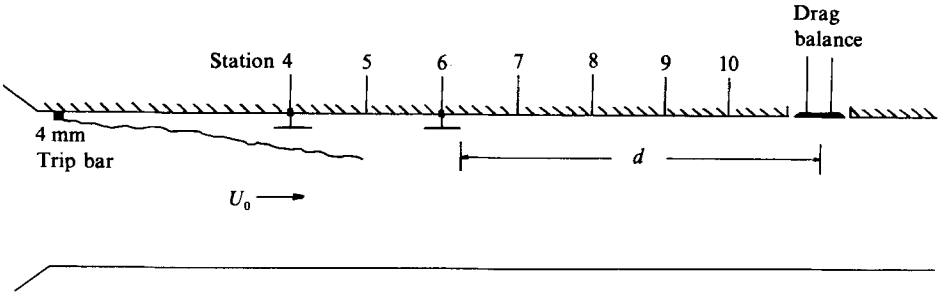

FIGURE 2. Wind-tunnel working-section geometry.

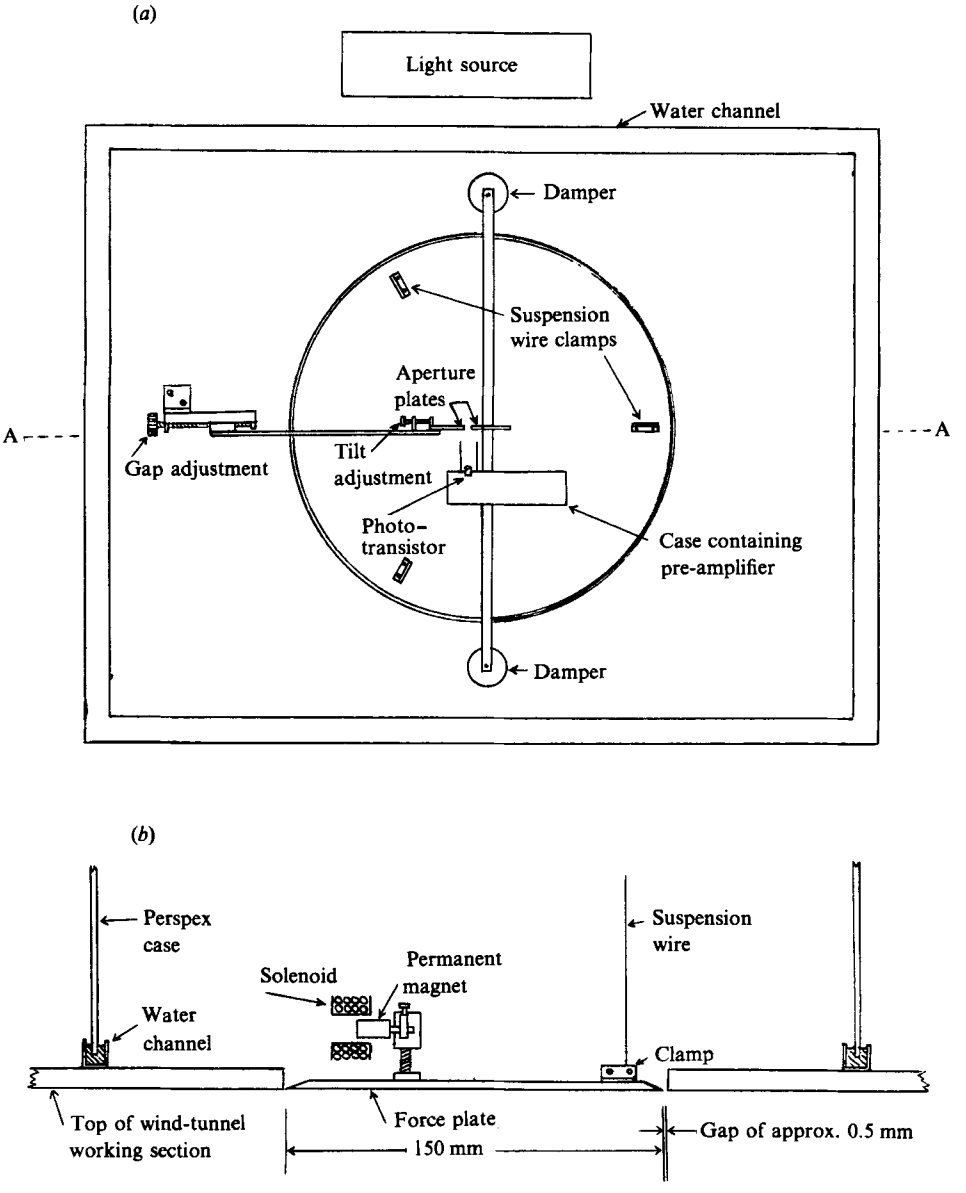

FIGURE 3. Skin-friction balance: (*a*) plan view; (*b*) elevation: section A–A.

(*a*) Centrifugal blower tunnel: $U_0 = 3.86$–11.2 ms^{-1} (7 velocities)
$Re_\theta = \approx 1000$–3500 (at device leading edge)

	Station 4	Station 6	Station 8	Station 9	Station 10
δ	27 mm	32 mm	37 mm	40 mm	42 mm
d/δ	56	34.5	19.5	12.5	7
Re_x	1.4×10^5	2.5×10^5	3.6×10^5	4.1×10^5	4.6×10^5

$Re_d = 5.4 \times 10^5 - Re_x$ (all for $U_0 = 3.86$ ms^{-1})

(*b*) Smoke-flow tunnel: $U_0 = 1.0$–2.4 ms^{-1} (3 velocities)
$Re_\theta = \approx 700$–1600

At equivalent Station 6:

Δ 85 mm Re_x 2.9×10^5	$U_{0\,(\text{visual})} = 1.0$ ms^{-1}, $Re_\theta \approx 700$
δ 82 mm Re_x 4.6×10^5	$U_{0\,(\text{camera})} = 1.6$ ms^{-1}, $Re_\theta \approx 1000$
δ 80 mm Re_c 6.9×10^5	$U_{0\,(\text{maximum})} = 2.4$ ms^{-1}, $Re_\theta \approx 1600$

TABLE 2. Comparison of flow parameters between the low-speed, smoke-flow suction tunnel and higher speed, centrifugal blower tunnel.

span, and obtaining the drag per unit width from the differences. The brass cylinder was selected to have the same device drag as the 3 in. plate (1.2 mm thickness) to allow a direct comparison of the skin-friction changes they produced as a result of the imposed momentum deficit. Seven tunnel velocities in the range 3.8–11.2 m/s were used, giving an Re_θ variation from 1000 to 3500, similar to earlier studies but the range of parameters covered was greater (see table 1).

The flow visualization was conducted in the 12 m $\times$ 0.91 $\times$ 0.91 m low-speed suction tunnel previously used by Head & Bandyopadhyay (1981). The tunnel and laser-sheet illumination have been described in detail by them. For the present studies suitably scaled versions of the plates and cylinder, all 0.9 m span, were mounted on the floor of the tunnel supported by adjustable legs at their extremities. The tripped floor boundary layer could be filled with smoke injected through a row of holes near the origin. Alternatively it was possible to introduce smoke more smoothly through a gauze-covered slot 450 cm downstream in order to look at the motion close to the wall in the disturbed layer.

This 'smoke' was actually a fine suspension of Shell Ondina oil produced by a smoke generator and this was illuminated either by two 1000 W tungsten iodide lamps or by a 5 W argon-ion laser. The fan-cooled white-light sources were mounted behind a thin slit in a reflecting box, on a trolley above the Perspex roof of the tunnel, and produced a beam approximately 8 cm wide. The illuminated region could be moved to any position along the tunnel: electric motor and mechanical drive systems allowed one to follow the developing flow and so record the relative motion in the convected view. The laser was fixed in an enclosed section beneath the tunnel, its beam fanned by a 5 mm glass rod into a plane 2 mm thick and directed up through the Perspex floor segment via a plane mirror. Although most of the views referred to here are longitudinal 'sections' of the flow, transverse and 45° inclined light planes have also been studied.

Three tunnel speeds were used (see table 2 for details and relevant parameters at the equivalent Station 6, 430 cm from the trip). Visual observations were made through the Perspex sidewall of the tunnel and still photographs taken with a Nikon f1.4 35 mm camera at 1/500 s (equivalent to 2 mm mean flow displacement). A motor

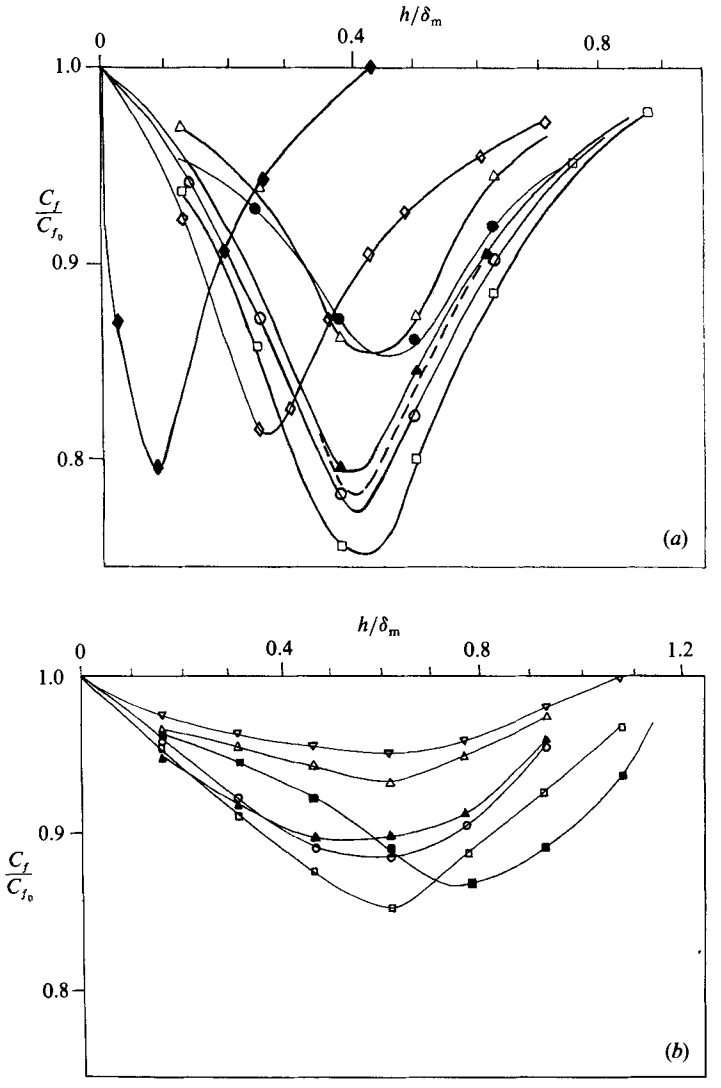

FIGURE 4. Effect of manipulator height on local skin-friction reduction for single flat-plate devices mounted at: (*a*) Station 9, $d = 12.5\delta$ ($t = 1.2$ mm, $Re_\theta = 1300$): △, $l = 0.65\delta$; ▲, $l = 1.3\delta$; ○, $l = 1.9\delta$; □, $l = 3.2\delta$; – – –, $l = 1.9\delta$ ($t = 0.56$ mm); ●, cylinder $D = 0.05\delta$; ◆, $d = 3\delta, l = 0.35\delta$; ◇, $d = 7\delta, l = 0.3\delta$ ($t = 0.4$ mm, $Re_\theta = 2100$, Nguyen *et al.* 1984*a*, *b*). (*b*) Station 6, $d = 34.5\delta$ ($t = 1.2$ mm, $Re_\theta = 1000$): ▽, $l = 0.2\delta$; △, $l = 0.8\delta$; ▲, $l = 1.6\delta$; ○, $l = 2.4\delta$; □, $l = 4\delta$; ■, $l = 4\delta$ ($Re_\theta = 2700$).

drive was added for sequences in the convected frame and cine films taken with a Bolex 16 mm reflex camera operating at 1/64 s. In all cases the film was Ilford HP5 uprated in Microphen to 3200 ASA or 800 ASA.

3. Results

3.1. *Skin friction*

Local skin-friction reductions as large as 33% were measured at the smallest distance (7δ) investigated downstream from the largest single plate when mounted close to the wall. This was comparable with other reported maximum values

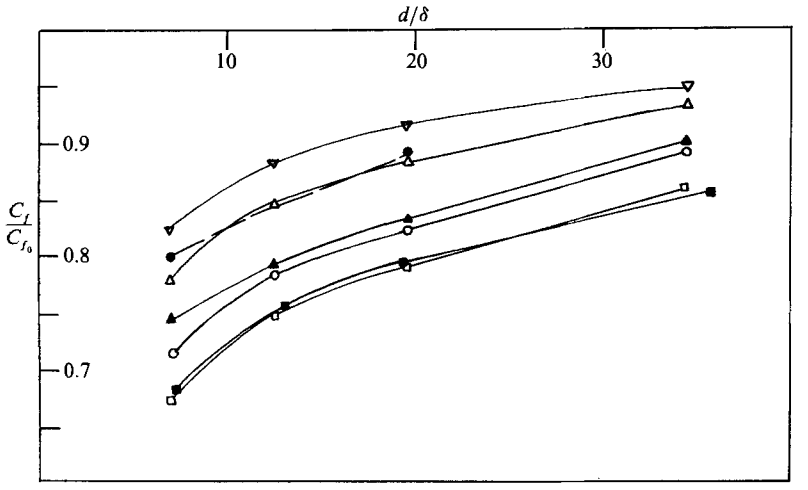

FIGURE 5. Variation of maximum local C_f reduction with distance downstream of the manipulators at $U_0 = 3.86$ m s^{-1}: ▽, $l = \frac{1}{4}$ in. plate; △, 1 in. plate; ▲, 2 in. plate; ○, 3 in. plate; □, 5 in. plate; —●—, cylinder; ■, 5 in. plate ($U_0 = 11.2$ m s^{-1}).

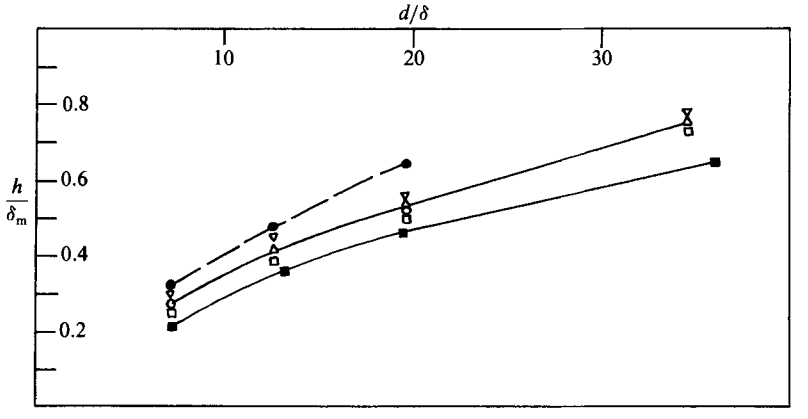

FIGURE 6. Height of manipulator required to achieve the maximum local C_f reductions plotted in figure 5 (symbols as for figure 5).

obtained at various distances behind a range of devices, but our results indicate that the magnitude of this peak reduction depended strongly on a combination of the location of the measuring position relative to the plate and the height of the latter, as well as its length and the free-stream velocity.

Representative data for plates positioned 12.5δ (Station 9) and 34.5 (Station 6) from the balance are presented in figure 4. These show the very large influence the height of the plate had on the reduction in C_f. This was particularly marked close behind the device where sharp minima were recorded but these became broader, and were reduced in magnitude, further downstream. The reduction did not show a simple variation with l. Instead there was a jump in performance near $l = \delta_m$. However, the effect of reducing the plate thickness by a factor of two, from 1.2 to 0.56 mm, was slight. The cylinder was only as effective as the 1 in. plate, except when mounted very close to the wall or near the outer edge of the layer.

Figures 5 and 6 show how the maximum C_f reduction increased as measurements were made progressively closer behind longer plates mounted nearer to the wall. At

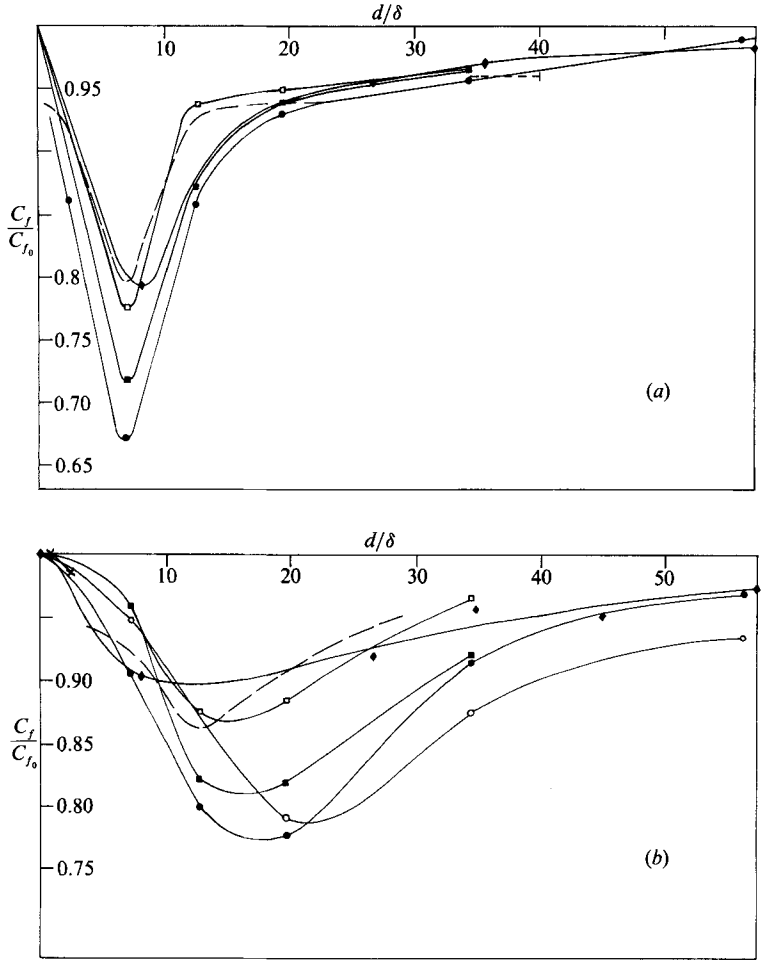

FIGURE 7 (*a*, *b*). For caption see next page.

a constant free-stream velocity, U_0, the height required to obtain the peak local C_f reduction at any given station was approximately the same for all plates, but as U_0 was increased it was necessary to move them closer to the wall. In each case the cylinder had to be positioned further out in the layer to achieve the same effect. Because the drag balance was fixed in position the manipulators had to be moved upstream to increase d, so l/δ_m and the tandem spacing, s/δ_m, varied inversely with x. For the 2 in. plate the boundary-layer growth resulted in a reduction in l/δ_m from 1.2 to 0.9 at Station 10 where figure 5 again indicates an associated drop in performance.

From a practical point of view one is more concerned with the skin-friction distributions generated downstream of devices mounted at fixed heights, and figures 7, 8 and 9 present the data in this form. Most of the results plotted are for $Re_\theta \approx 1000$ to allow direct comparison with the smoke flow visualization.

Although the large C_f reductions obtained with single plates mounted at $h = 0.25\delta$ look impressive it is the area under these curves that is important in assessing the net drag. The fact that the local reduction was not sustained, but fell off rapidly, with the flow essentially recovering from the perturbation in 75δ, meant that the drag performance was actually rather poor. For example the total skin-friction reduction

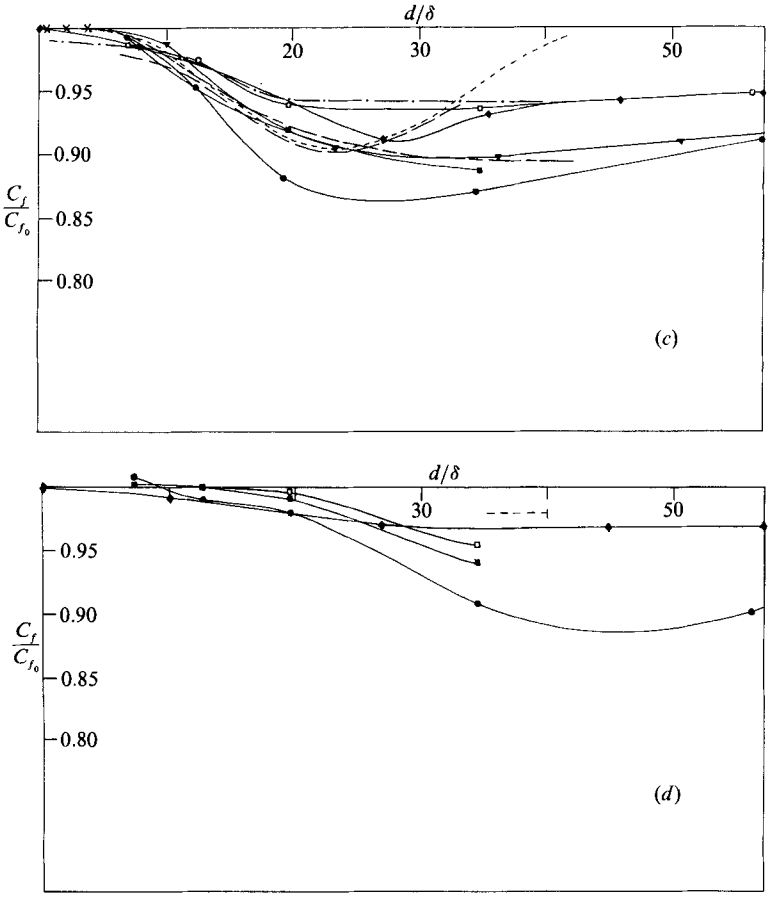

FIGURE 7. Skin-friction distributions downstream of single plates or cylinders mounted at fixed heights: (*a*) $h = 0.25\delta$ ($t = 1.2$ mm, $Re_\theta = 1000$): □, 1 in. plate, $l = 0.6\delta$–0.8δ; 3 in. plate, $l = 1.8\delta$–2.4δ; ●, 5 in. plate, $l = 3.0\delta$–4.9δ; ——, cylinder $D = 0.05\delta$–0.07δ; ◆, $h = 0.32\delta$, $l = 0.95\delta$, $t = 0.4$ mm, $Re_\theta = 2100$ (Lemay *et al.* 1985); – – – –, $h = 0.2\delta$, $l = 0.8\delta$, $t = 0.254$ mm, $Re_\theta = 2500$ (average reduction over 40δ, Hefner *et al.* 1983). (*b*) $h = 0.5\delta$ ($t = 1.2$ mm, $Re_\theta = 1000$): symbols as for (*a*) but with: ○, 5 in. plate, $l = 3.3\delta$–5.2δ, $Re_\theta = 2700$; ◆, $h = 0.48\delta$; ×, $h = 0.4\delta$, $l = 0.8\delta$, $t = 0.14$ mm, $Re_\theta = 4000$ (Sandborn 1981). (*c*) $h = 0.75\delta$ ($t = 1.2$ mm, $Re_\theta = 1000$): symbols as for (*a*) but with: ◆, $h = 0.75\delta$ and ▼, $h = 0.75\delta$, $l = 1.3\delta$, $t = 0.25$ mm, $Re_\theta = 3700$ (Westphal 1986). $h = 0.8\delta$: ×, $l = 0.8\delta$, $t = 0.14$ mm, $Re_\theta = 4000$ (Sandborn 1981); ——·—, $l = 1.6\delta$, $t = 0.1$ mm; ——·, $l = 0.8\delta$, $t = 0.1$ mm; – – – –, cylinder $D = 0.08\delta$, $Re_\theta = 2500$ (Takagi 1983*b*). (*d*) $h = \delta$ ($t = 1.2$ mm, $Re_\theta = 1000$): symbols as for (*a*) but with ◆, $h = 1.02\delta$; – – – –, $h = \delta$.

with the 1 in. plate (□) would have amounted to only an average of 4 % C_f reduction over 80δ, in close agreement with the early NASA result using a much larger size balance. However this again shows the advantage of more local measurements because such integration of the skin friction over a large area smears out the C_f minima and obscures the details of the distributions.

When the plates were mounted at $h = 0.5\delta$ the maximum C_f reduction occurred later and was smaller (23 % for the longest plate). However the recovery process was more gradual and there was thus the possibility of a larger integrated skin-friction reduction particularly at higher U_0, Re_θ when, as indicated for the longest plate, the peak reduction was delayed and the whole distribution skewed downstream. When mounted at the same height the cylinder performed considerably worse than the

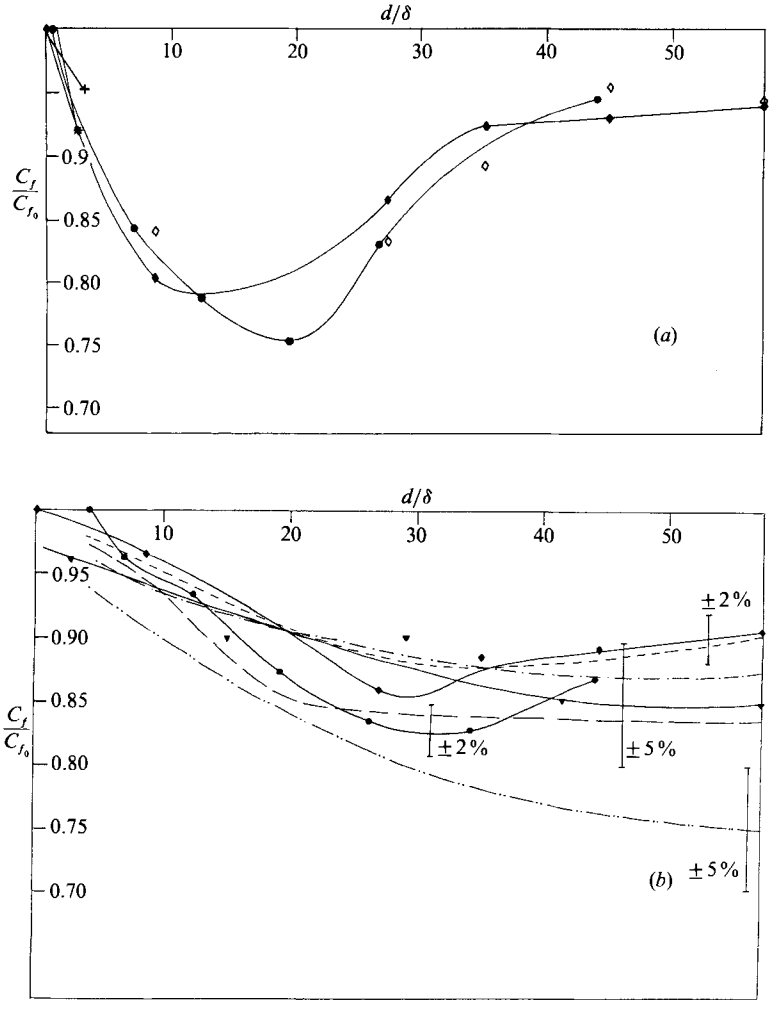

FIGURE 8. Skin-friction distributions behind tandem plates mounted at: (*a*) ●, $h = 0.5\delta$, $l = 1.5\delta$–2.2δ, $s = 4.9\delta$–7.1δ, $t = 1.2$ mm, $Re_\theta = 1500$; ◆, $h = 0.48\delta$, $l = 0.95\delta$, $s = 5.1\delta$, $t = 0.4$ mm, $Re_\theta = 2100$ (◇, Preston-tube data; Lemay *et al.* 1985). $h = 0.4\delta$: *, $s = 1.6\delta$; +, $s = 3.2\delta$; $l = 0.8\delta$, $t = 0.14$ mm, $Re_\theta = 4000$ (Sandborn 1981). (*b*) $h = 0.75\delta$: symbols as for (*a*) and with: —— ·, $l = 0.5\delta$, $t = 0.15$ mm; —— · ·, $l = 1.5\delta$, $t = 0.05$ mm, $s = 5\delta$, $Re_\theta = 3800$ (Bertelrud *et al.* 1982); ▼, $l = 1.3\delta$, $s = 7.1\delta$, $t = 0.25$ mm, $Re_\theta = 3700$ (Westphal 1986). $h = 0.8\delta$: – – –, $l = 0.7\delta$, $t = 0.05$ mm; ——, $l = 1.4\delta$, $t = 0.1$ mm; $s = 6.6\delta$, $Re_\theta = 3000$ (Takagi 1983*a*).

3 in. plate. A comparison of figure 7(*b*) with figure 8(*a*) shows that two 2.5 in. plates in tandem ($l \sim 2\delta$, $s \sim 5\delta$) produced a slightly larger peak and integrated C_f reduction than the single 5 in. plate, but it should be noted that the improvement in the initial region was because the origin was taken as the trailing edge of the second plate so that there was already some contribution from the first plate further upstream by this stage.

Raising the devices to $h = 0.75\delta$ further delayed the point of maximum local skin-friction reduction and this reached only 13% for the 5 in. plate. The tandem plates however then produced a considerably larger (18%) reduction at a later stage of development as indicated in figure 8(*b*), and this lower level persisted for longer.

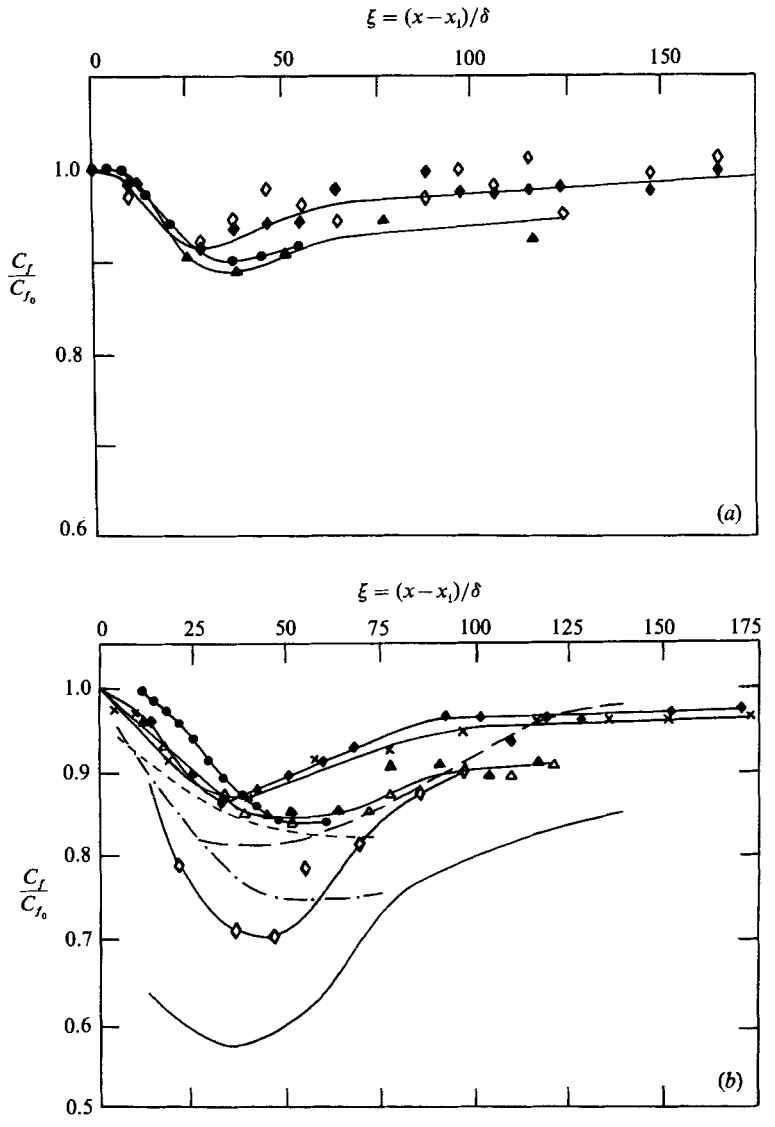

FIGURE 9. Extended skin-friction distributions far downstream of manipulator devices. (*a*) Single plates: ●, $l = 1.3\delta$–2.0δ, $h = 0.75\delta$, $t = 1.2$ mm, $Re_\theta = 1900$–3100; ◆, $l = 0.95\delta$, $h = 0.75\delta$, $t = 0.4$ mm, $Re_\theta = 2100$ (◇, Preston-tube data; Lemay *et al.* 1985); ▲, $l = 1.3\delta$, $h = 0.75\delta$, $t = 0.25$ mm, $Re_\theta = 3700$ (Westphal 1986). (*b*) 'Optimized' tandem devices; ●, $l = 1.6\delta$–2.4δ, $s = 5.3\delta$–7.9δ, $h = 0.75\delta$, $t = 1.2$ mm, $Re_\theta = 1900$–2900; ◆, $l = 0.95\delta$, $s = 5.1\delta$, $t = 0.4$ mm, $h = 0.75\delta$, $Re_\theta = 2100$ (Lemay *et al.* 1985); ▲, $l = 1.3\delta$, $s = 7.1\delta$, $h = 0.75\delta$, $t = 0.25$ mm, $Re_\theta = 3700$ (△, C_f from log law; Westphal 1986); ×, $l = 1.0\delta$, $s = 6.5\delta$, $h = 0.75\delta$, $t = 0.25$ mm, $Re_\theta = 3000$ (Stanton-tube data, Haritonidis, Landahl & Widnall 1985); – – –, $l = 0.8\delta$, $s = 6.4\delta$, $h = 0.8\delta$, $t = 0.254$ mm, $Re_\theta = 2300$ (Hefner *et al.* 1983); ————, $l = 1.0\delta$, $s = 5\delta$, $h = 0.8\delta$, $t = 0.254$ mm with tapered trailing edge, $Re_\theta = 3300$ (Anders *et al.* 1984); —— ·, $l = 1.4\delta$, $s = 5.9\delta$, $h = 0.68\delta$, $t = 0.15$ m, $Re_\theta = 3000$ (Veuve & Truong 1984); ——, average curve of several data sets with: $l = 1.9\delta$, $s = 14\delta$, $h = 0.68\delta$, $t = 0.1$ mm, $Re_\theta = 2900$ or $l = 1.1\delta$, $s = 11\delta$, $h = 0.5\delta$, $t = 0.1$ mm, $Re_\theta = 4900$ (Plesniak & Nagib 1985); ◇, $l = 1.2\delta$, $s = 5\delta$, $h = 0.8\delta$, NACA 0009 aerofoil section manipulators, $Re_\theta = 7400$ (Anders & Watson 1985).

Finally when the plates were moved up to the top of the boundary layer it took longer for their influence to penetrate to the wall and there was some evidence that small increases in C_f occurred close behind the manipulator before any reduction took place.

Recently, Nguyen, Savill & Westphal (1987) have compared results from three independent manipulator experiments where direct local skin-friction measurements have been obtained using either a drag balance, as in the present experiment and those of Mumford & Savill (1984); Nguyen *et al.* (1984*a*, *b*); Lemay *et al.* (1985), or an oil film interferometer (Westphal 1986), and found very good agreement regarding the skin-friction distribution behind a single plate and a tandem configuration. This comparison is extended here by plotting further results from these other 'direct' investigations, together with some of the limited data from Sandborn (1981) on to figures 7 and 8. For single plates with an l/δ of approximately either 0.9 or 1.5 there is excellent agreement on the magnitude and shape of the skin-friction distribution and the manner in which this varies with h/δ. This is particularly so when allowance is made for small differences in the plate parameters l/δ, h/δ, variations in Re_θ, and also for the fact that the 4δ streamwise extent of our balance artificially smoothed the C_f curves slightly compared to the smaller ($\sim \delta$) balance used by Nguyen *et al.* and point measurements from the oil-film interferometer and surface-mounted hot wires. By analysing anemometer data in conjunction with the direct measurements of u_τ, Nguyen *et al.* (1987) have shown that the universal law of the wall is rapidly re-established (within $\sim 15\delta$) in such flows, so a comparison is also made with some of the previous measurements using wall similarity techniques which rely on the existence of the law of the wall. The results obtained by Takagi (1983*b*), using a Preston tube, behind both a single plate and a cylinder are included in figure 7(*c*). Again there is remarkably good agreement with our curves for the 1 in. and 3 in. plates and the cylinder with the same device drag. The influence of plate thickness over the range from 1.2 mm to 0.1 mm appears to be minimal.

The results of Nguyen *et al.* (1984*a*, *b*); Lemay *et al.* (1985) for tandem plates with $s = 5\delta$ and at a similar Re_θ confirm the similarities and differences we observed in shape, magnitude and variation with h/δ of the C_f distributions to those found behind single plates. Their C_f minimum in figure 8(*a*) occurs before ours, but one would expect this because their plates were mounted a little closer to the wall. When both pairs of tandem plates were mounted at $h/\delta = 0.75$ the minima were virtually coincident and the two C_f curves shown in figure 8(*b*) are virtually parallel for most of their length. The difference in magnitude is consistent with the earlier observation of a jump in performance between l less than δ_m and l greater than δ_m. The discrepancy near the trailing edge of the second plate is probably a result of the finite thickness of the plates and the associated variation in their influence on the wall static pressure beneath them with t as discussed by Savill (1986). A similar effect of l/δ is seen in the data of Bertelrud *et al.* (1982: Preston tube) and of Takagi (1983*a*: Clauser Plot), and the remaining curves divide into two sets: those for plates with $0.5 \leqslant l/\delta \leqslant 0.8$, which are in broad agreement with Nguyen *et al.* (1984*b*), and those for $l/\delta \approx 1.5$, which straddle the present results. At first sight it would appear that there is rather more scatter in the latter, but one should make allowance for the shift in minima downstream with increased Re_θ. Overall the agreement is probably within the available estimates of experimental uncertainty.

One can see then that the flow velocity and height of the device element(s) determine (with s) the shape and magnitude of the C_f distributions. The closer the lowest element to the wall the quicker and the larger the local C_f reduction, but also

the more rapid the onset of recovery. Accordingly it seems that one should be looking for the type of flattened distributions found when $h = 0.75\delta$ in order to maximize the integrated skin-friction saving, and hence net drag benefit, provided these persist downstream. As indicated in figure 9(*b*), which is based on a compilation due to R. V. Westphal (private communication), subsequent measurements have now shown that this reduction does indeed persist for at least approximately 120δ from the device and Lemay *et al.* (1985) have shown by an area integration of curves for different h/δ that a value of h equal to 0.75δ is optimum for both single and tandem plates at an Re_θ of about 2000. However from the above analysis it would seem advisable to position devices closer to the wall in order to obtain the optimum performance at higher Re_θ, as indeed Veuve & Truong (1984: $h = 0.68$ at $Re_\theta \approx 3000$) and Plesniak & Nagib (1985: $h = 0.68$ at $Re_\theta = 2900$; $h = 0.5$ at $Re_\theta = 4900$) have done.

3.2. *Device drag and net reductions*

The total device drag (skin friction + form drag) in N/m span/$(\mathrm{ms}^{-1})^2 \times 10^{-3}$ for the single, rectangular section, 1.2 mm thick plates mounted at $h = 0.75\delta$ were as follows: 1 in. plate (2.8); 2.5 in. plate (3.5); 5 in. plate (4.9) corresponding to drag coefficient of 0.18, 0.09 and 0.063 respectively. The drag was proportional to U_0^2 so the absolute value would have been reduced as the plates were moved closer to the wall. There was no evidence for the device-drag minimum near $h = 0.3\delta$ reported by Hefner *et al.* (1979). For the range of lengths investigated a plate thickness of 1.2 mm resulted in a form-drag contribution which was a significant fraction of the total, but was approximately independent of plate length. The variation of skin-friction coefficient with distance from the leading edge of the plate which has been discussed by Hoerner (1965) was responsible for the observed decrease in drag per unit length with increase in l. Raising l from 2.5 to 5 in. resulted in a 40% increase in drag penalty, a figure identical to that obtained by Takagi (1983*a*, *b*). By comparison similar measurements of the 2.5 in. plates in tandem indicated that the drag of the second element was only reduced to $\approx 85\%$ of its unshielded value. This was a noticeable saving compared to the other twin plate arrangements, but considerably worse than if the two plates were merely joined together. It is not therefore obvious that the tandem configuration is best. For it to prove better than a single unit of the same total length it must produce a significant improvement in the magnitude and extent of the C_f reduction. In view of their greater drag penalty one could virtually rule out triple and multiple stacked devices, and probably even twin stacked and staggered arrangements, as contenders for net drag-reduction devices.

The thickness of our devices precluded any serious attempt at achieving such net benefits and the minimum net drag over the available development length amounted to a 36% increase. Even when they were reduced in thickness to $t = 0.56$ mm, form drag accounted for $\approx 30\%$ of the device drag and other results suggest it would be necessary to reduce them to ≈ 0.1 mm thick in order to restrict this to just laminar skin friction. Also we were only able to study quantitatively the first 60δ behind the device and so could not evaluate the total integrated skin-friction reduction to set against the device drag. However, over this region as indicated in figure 9(*a*, *b*), our results do follow very closely the curves for similar configurations of both single and tandem plates obtained by Lemay *et al.* (1985), Westphal (1986) and Anders, Hefner & Bushnell (1984: momentum balance) whose measurements have been extended sufficiently far downstream to perform such an integration. If the plate efficiency does not fall off appreciably with t until at least $t = 0.1$ mm, as appears to be the case from the comparisons made in figures 7 and 8, and if we extrapolate our results in line

with their data these support their estimates of a 2% net reduction for a single plate ($l \approx \delta$); 4% for a tandem ($l \approx \delta$, $s \approx 5\delta$) over a distance of 120δ. By increasing s to 10δ, and tapering the trailing edges of their devices, Anders *et al.* (1984) improved their net gain to 7%. The results obtained more recently by Veuve & Truong (1984: Preston tube) and Plesniak & Nagib (1985: momentum balance) suggest that much larger skin-friction and net drag reductions are attainable using carefully set up, thin, tensioned elements at higher Re_θ, Re_l.

Such fragile manipulators would necessarily be replaced by stronger, self-supporting, aerofoil-section devices for practical applications. Anders & Watson (1985) have shown that a net drag reduction of 7% can also be achieved with tandem NACA 0009 aerofoil manipulators in place of the thin elements used for their earlier investigations (a comparison is made in figure 9*b*). However Anders (1986) has pointed out that both these studies, and indeed all of those referred to in the present work, were strongly influenced by low-Reynolds-number effects. It is therefore questionable whether the optimum parameters deduced from these will be relevant to practical applications of such devices in flight. Flight test data reported by Bertelrud (1984, 1986) indicate that equivalent C_f reductions can be obtained with similarly scaled profiled manipulators. However such use of aerofoils at high Reynolds numbers has emphasized the importance of other parameters including the profile shape, angle of attack, and chord Reynolds number, all of which need to be optimised to maximize the net effect, and has even raised the question of whether a single device might be sufficient when its boundary layers are fully turbulent.

3.3. *Flow visualization*†

The flow visualization supported the picture of the boundary layer presented by Head & Bandyopadhyay (1981) which has received earlier corroboration from Wallace *et al.* (1983) and Perry & Chong (1982) among others. The flow approaching the manipulators was composed of large bulges each of which contained a group of hairpin vortices typically inclined at approximately 45° to the flow direction, but slowly overturning *en masse*. Their tops in cross-section appeared as transverse vortices responsible for entrainment by small-scale 'nibbling' of the turbulent–irrotational interface predominantly on the upstream face of the bulge. The pictures shown in figure 10 are an idealized representation based on visual, and photographic records examples of which are provided by figure 11. In practice all the hairpin eddies were distorted by the velocity fields of their neighbours and near the wall, tangling and subsequent vortex breakdown generated large numbers of small-scale eddies.

Figure 10(*a*) and (*b*) shows the situation when a single plate, $l = 1.8\delta_m$, (equivalent to the 3 in. plate of Station 6) was mounted first at $h = 0.75\delta$ and then $h = 0.25\delta$. As the flow reached the device it moved outwards ($\delta_m \approx 1.3\delta$). The tops of the tallest hairpins passed over the obstruction, they became wrapped around the leading edge and were finally cut in two. The top parts, which sometimes reformed as vortex rings, were thus set free from the restraining influence of the wall and moved off rapidly downstream where they bunched up, smoothing the interface. The truncated lower sections and shorter hairpins continued to rotate as they passed beneath the plate, but appeared to be ordered by it. Hairpin production continued, but became more regular.

† Throughout the paper the flow is described as if the boundary layer were developing on the floor of the tunnel.

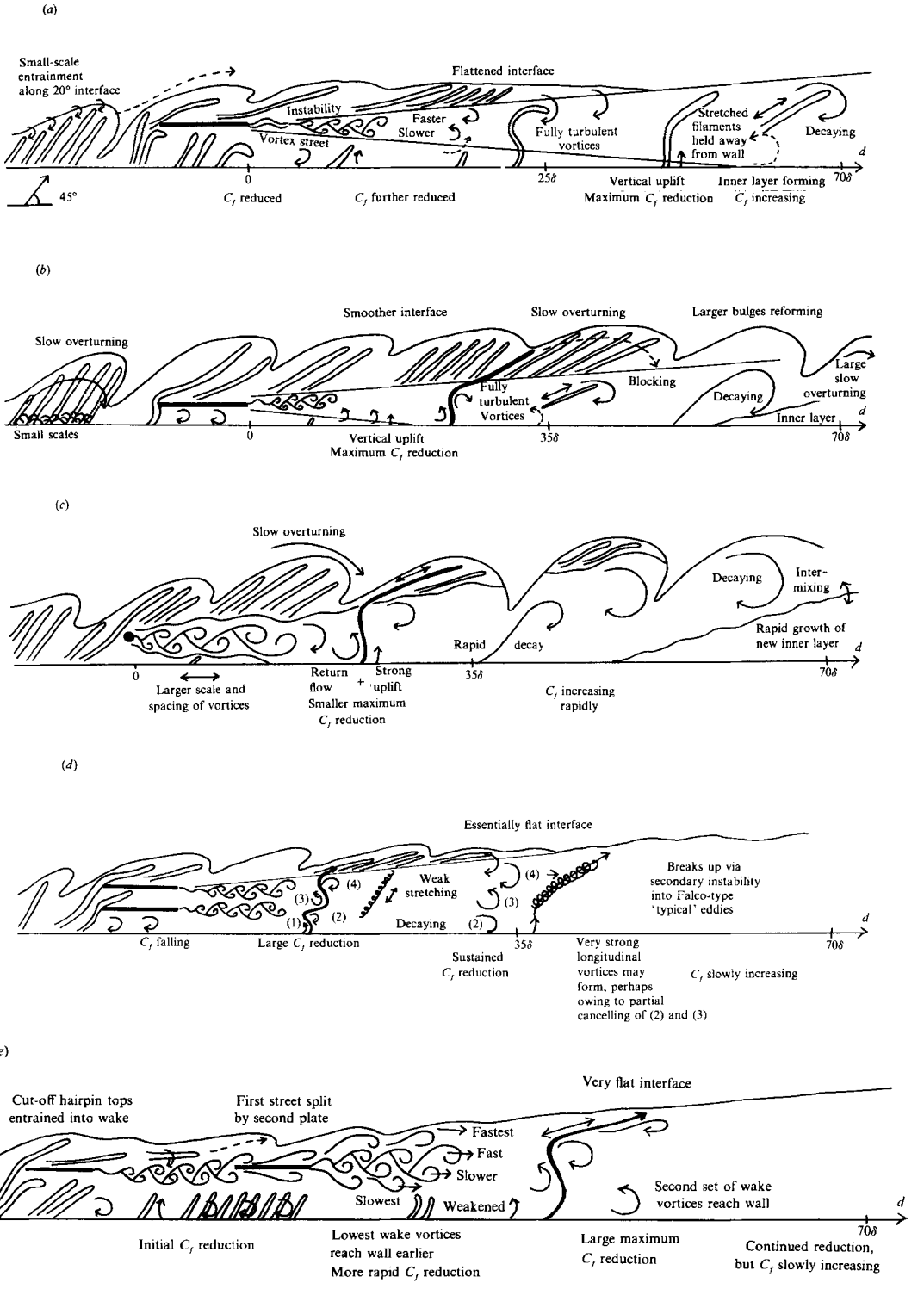

FIGURE 10. Schematic pictures of boundary-layer manipulation based on flow visualisation. (*a*) Single plate: $l = 1.8\delta_m$, $h = 0.75\delta$. (*b*) Single plate: $l = 1.8\delta_m$, $h = 0.25\delta$. (*c*) Cylinder: $D = 0.05\delta_m$, $h = 0.5\delta$. (*d*) Twin stacked plates: $l = 1.8\delta_m$, $h = 0.3\delta$, 0.6δ. (*e*) Twin tandem plates: $l = 1.8\delta_m$, $s = 5\delta$, $h = 0.75\delta$.

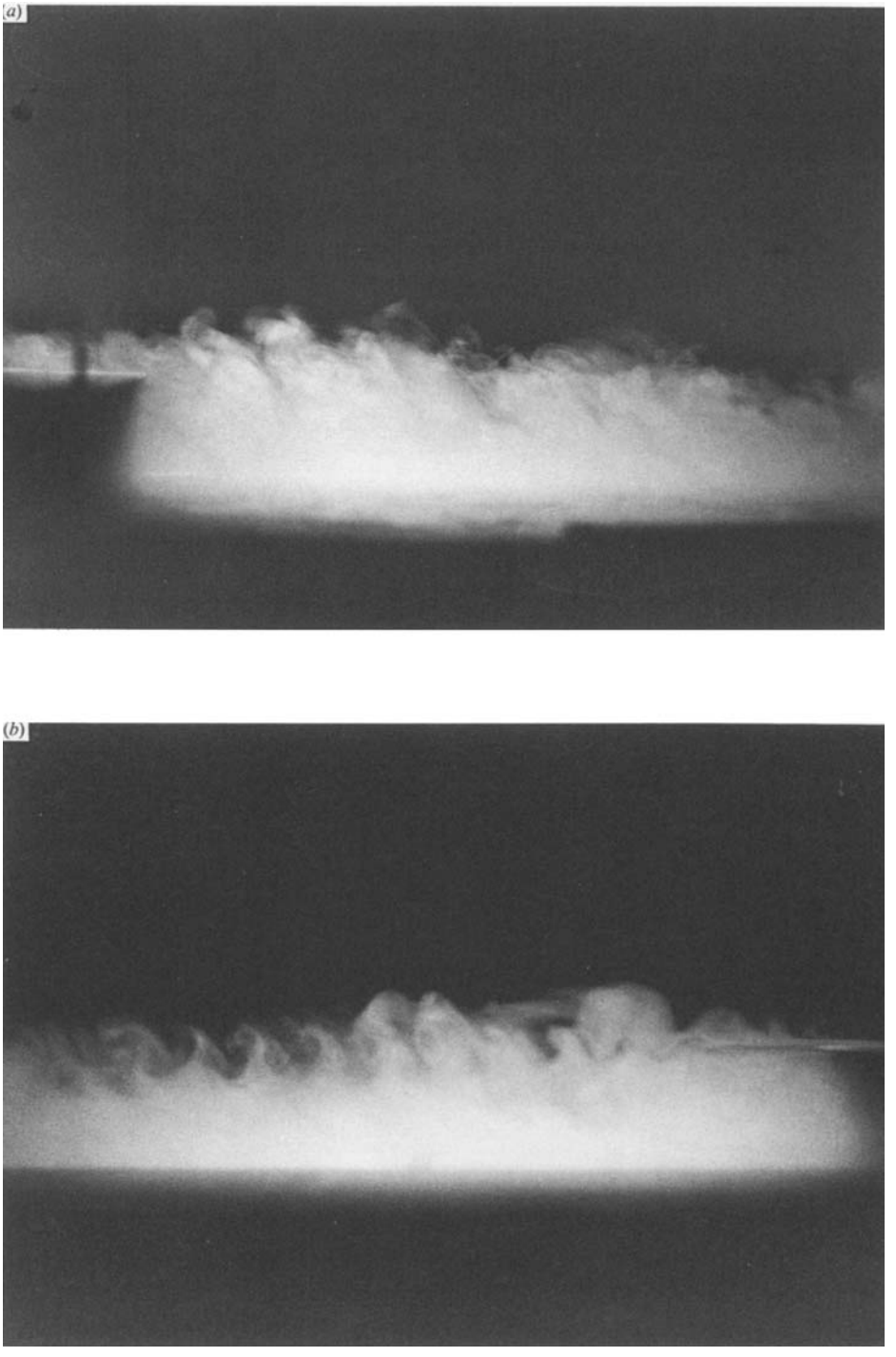

FIGURE 11 (*a*, *b*). For caption see page 409.

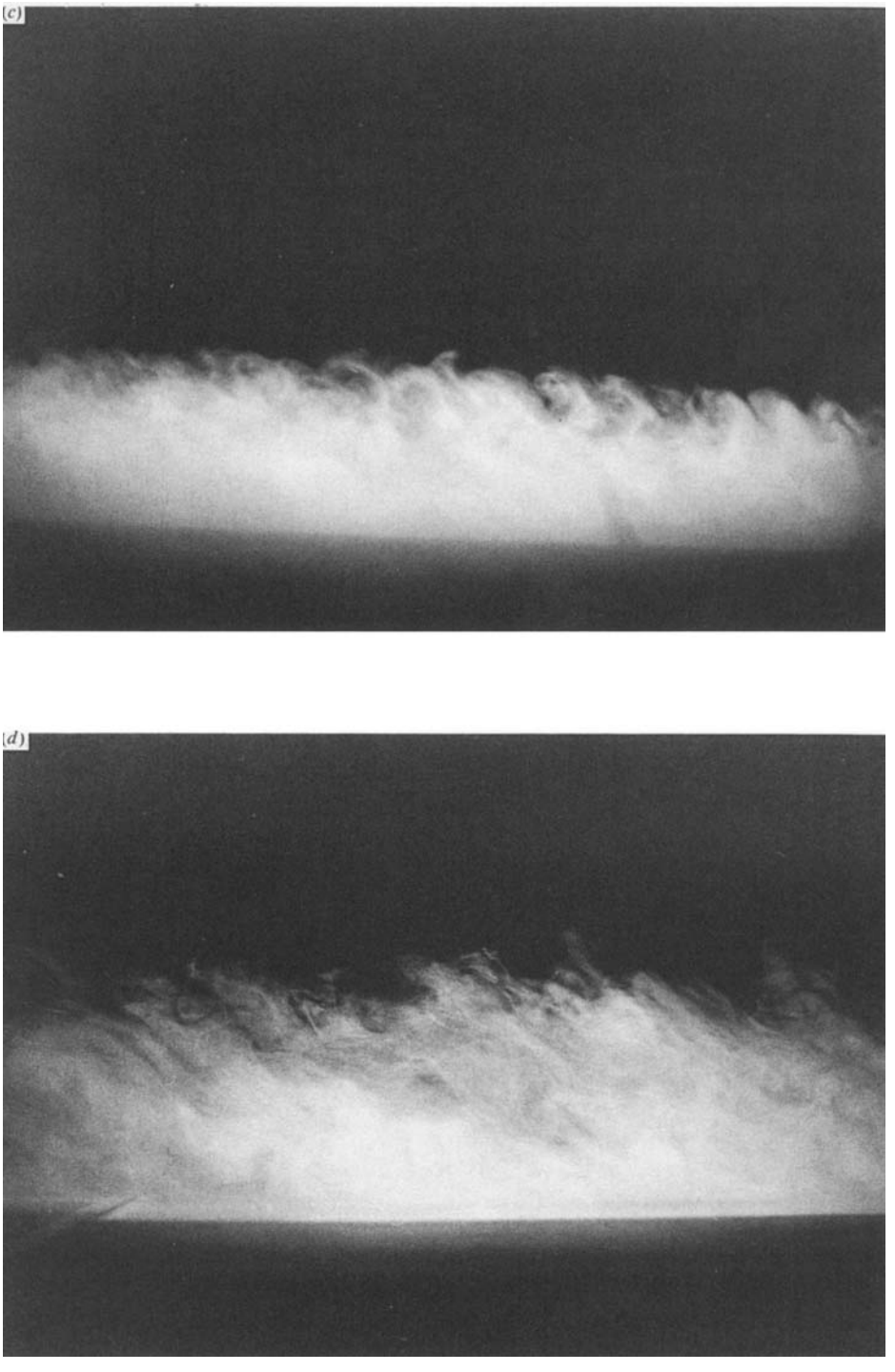

FIGURE 11 (*c*, *d*). For caption see page 409.

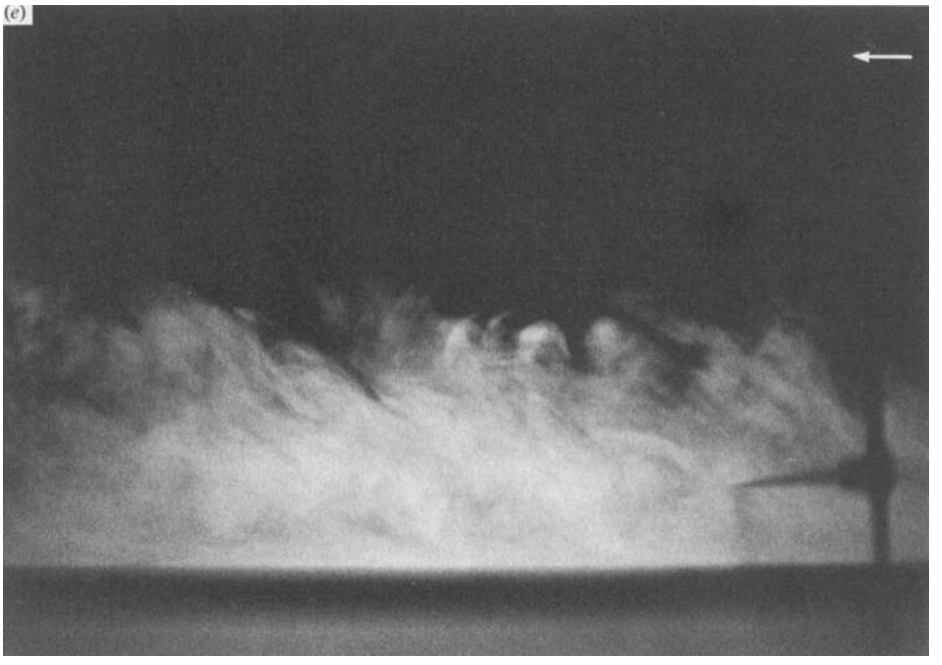

FIGURE 11. (*a*) Boundary layer approaching single-plate manipulator, $l = 1.8\delta_m$, $h = 0.8\delta_m$, $Re_\theta = 1000$. (*b*) Manipulated boundary layer immediately downstream of single-plate device, $l = 1.8\delta_m$, $h = 0.8\delta_m$, $Re_\theta = 1000$. (*c*) Manipulated layer approximately 25δ downstream of single plate, $l = 1.8\delta_m$, $h = 0.8\delta_m$, $Re_\theta = 1000$. (*d*) Manipulated boundary layer approximately 50δ downstream of single plate, $l = 1.8\delta_m$, $h = 0.8\delta_m$, $Re_\theta = 1000$. (*e*) Boundary layer immediately downstream of circular cylinder manipulator, $D = 0.05\delta_m$, $h = 0.5\delta_m$, $Re_\theta = 1000$.

Behind the plate an initially laminar instability rapidly (within δ) broke down to form a compact vortex-street wake composed of fast spinning vortices which remained essentially fully coherent for about 6δ, but retained most of their circulation and persisted for more than 70δ. This wake separated the two regions of boundary-layer structures and seemed to block high-speed irrotational fluid, and the outermost turbulent motions, from directly influencing the wall region as Bertelrud *et al.* (1982) have conjectured. The top set of wake vortices absorbed the decaying outer hairpin section and then formed the interface which remained relatively flattened because they were much smaller in scale and spacing than the original bulges.

As the lower wake vortices moved down through the layer they induced a more vertical uplift of material away from the wall. At this stage, smoke introduced through the gauze was convected up across the wake centreline and was rapidly transported to the outside of the flow by the wake vortices, following characteristic 'S'-shaped paths, When the lower set reached the sublayer the uplift of new hairpins from the top of this layer became essentially vertical. This occurred precisely in the region where the maximum drag reduction had been recorded (near $d = 35\delta$ in this case). We prefer to regard this interaction between the lower wake vortices and the near-wall structure as a cooperative one, but one could equally consider the former simply as countervorticity components which act to cancel some of the mean vorticity at the wall, the interpretation adopted by Anders *et al.* (1984).

As a result of the mean shear the top set of wake vortices moved faster than the

lower set so the drawn-up vortex loops became stretched out as filaments in the wake and so were held away from the wall as they were convected downstream. The lower set of vortices then impinged on the wall, were weakened, and decayed. Once this occurred a new internal layer began to form and this grew slowly outwards as the outer wake vortices also decayed. Presumably complete recovery would not occur until the strength of these eddies fell below that of the new hairpins. The available development length was insufficient to see this final stage in the recovery process, but interfacial bulges began to reappear approximately 70δ downstream of the plate. Eventually the edge of the inner layer should reach the turbulent–irrotational interface and the normal boundary-layer structure be re-established.

When the plate was placed lower in the layer, as in figure 10(*b*), virtually all the hairpins were cut through, but the upper sections retained their collective motion and it took longer for the upper edge of the wake to reach the interface so this remained irregular. The lower wake vortices now reached the wall earlier, while they were stronger, again at a point coincident with the observed maximum local skin-friction reduction, which was then larger. The wake was now also effective in blocking the slow overturning in the outer region, as well as the influence of smaller scale fluctuations there, and preventing incursions of external irrotational fluid to the wall. The decay of the inner wake vortices was more rapid and the internal layer began to form by 50δ. Interfacial bulges also reformed more rapidly and this process seemed to be stimulated by the presence of the outer wake vortices with the same sign of circulation, but there appeared to be little mixing across the internal boundary. Again full recovery did not occur within the development length of the tunnel.

A shorter plate, $l \approx 0.3\delta_m$ presented essentially the same picture as the longer one, but the initial instability at the trailing edge was shorter and the vortex street contained smaller, more compact, vortices which were closer spaced (all scales were related to both t and l)†. Although these street vortices and their fully turbulent counterparts appeared just as persistent they influenced a smaller region of the boundary layer and the plate was less effective at interrupting the hairpins' collective rotation, particularly when placed high in the layer. When mounted close to the wall ($h \leqslant 0.5\delta$) the plate wake was perturbed by the outer layer motions and so did less to shield the near-wall flow from their influence.

For comparison figure 10(*c*) shows the situation when a cylinder with the same drag as the longer plate was mounted at $h = 0.5\delta$. This generated a more vigorous, larger-scale vortex street. The lower set reached the wall quickly and produced a strong uplift, but they were then equally rapidly suppressed by the wall. The outer wake vortices were still strong at this stage and being larger scale produced undulations in the turbulent–irrotational interface. They also stimulated intermixing with the structures in the internal layer, promoting a more rapid growth of the new layer. Blocking was similarly short-lived and apparently rendered less effective by the fact that the wake vortices were sufficiently widely spaced for the upper set to adversely affect the inner boundary-layer region.

When two $l = 1.8\delta_m$ plates were mounted one above the other they were more effective at suppressing the collective motion and their two wakes acted initially independently so that the smoke tracer which was lifted away from the wall by the vortices in the bottom wake was carried on up through the layer by those in the top wake, following a complex path to the external boundary (see figure 10*d*). At the

† The scale of the vortices depended on t and the thickness, at the trailing edge, of the boundary layer developing along the plate.

same time they appeared to act as two separate 'shields', the lower one reinforcing the blocking action of the upper. Again because of the mean shear there was a tendency for lifted vortex loops to be stretched into the stream direction in the upper part of the flow. The lowest set of wake vortices (1) quickly interacted with the wall and died away. Further downstream the other sets were also decaying, but by this stage the two wakes were themselves interacting and occasionally the counter-rotating elements (2) and (3) appeared to cancel one another. Then any vorticity which was preferentially aligned between the outermost set (4) and the wall was greatly stretched and amplified to produce intense inclined longitudinal vortices which underwent a secondary instability forming large numbers of structures similar to the 'typical eddies' of Falco (1979). There was an indication that material continued to be uplifted into the cores of these remarkable structures, which have also been observed in wake/boundary-layer interactions by Savill & Zhou (1983).

The effect of staggering the top plate either upstream or downstream was investigated, but the general picture was essentially the same as with vertical stacking. With an upstream stagger the upper wake was already developed before the second one formed so that by the time the latter began to affect the mean wake flow the two wakes were already interacting. This led to a rather confused motion and reduced the strength of the upper wake's vortices. A downstream stagger held more promise because of the delayed initiation and spreading of the top wake. Hefner *et al.* (1979) observed a double minimum in the C_f distribution behind such a configuration and it would seem from the other observations reported here that this could be connected with the order in which the different sets of wake vortices interacted with the near-wall flow. However it is possible that the main effect of their $\pm 60°$ stagger was to increase the 'effective length' of their plates. A downstream stagger of $\leqslant 45°$ appeared to be a better prospect because the plates then directly influenced a larger proportion of the hairpins composing any one bulge, destroying their combined larger-scale motion and chopping them into smaller sections.

A tandem arrangement is depicted in figure 10(*e*). When the vortex street formed behind the first plate impinged on the second it split so that the top set of vortices passed over the second plate and the lower set below it. Their presence appeared to amplify the instability at the trailing edge, producing a larger-scale second street. This lay embedded in the first so that there were again four sets of vortices arranged vertically as with the stacked and staggered cases, but now a second set of more intense counterrotating or uplifting vortices lay directly above the lowest set of such structures. This appeared to be the most advantageous arrangement because the first set were displaced towards the wall by the second stronger set and so reached it sooner. Then when they decayed the latter took over their role and it was at that point that the maximum drag reduction had been detected with this configuration.

4. Discussion

The flow visualization immediately showed that the wake of the manipulator plates can play a far more important role than had previously been appreciated. Many researchers have taken the view that the bulges of the undisturbed boundary layer represent physical large eddies responsible for entrainment of external irrotational fluid by large-scale overturning, and have assumed that flat-plate devices work principally by destroying or suppressing these eddy structures by restricting vertical fluctuations and introducing small scales into the flow to initiate a forced energy cascade. The latter was regarded as the main influence of the wake

by Corke *et al.* (1982) although they have also suggested that a transfer of energy from the turbulence to the mean flow in the lower half of the wake, partly balanced by excess production in the upper half, might play a role in reducing the level of turbulent intensity in the layer below the level of the plate. Hefner *et al.* (1979) have proposed a 'vortex unwinding' mechanism whereby such incoming large eddies might generate cancelling starting vortices as they are convected past the plate. The implication of this picture is that the changes to these large scales ensure that high-speed sweeps of potential fluid no longer impinge on the sublayer, damping bursting and reducing C_f. At the same time such an interpretation is consistent with the measured reduction in entrainment and observed flattening of the turbulent–irrotational interface behind the device.

However, the observation that the large bulges are merely collections of hairpin vortices is an aspect that has yet to be incorporated into this explanation of how such devices work. If one accepts that these are the dominant energy-containing 'large eddies', and that any larger, predominantly transverse scales of motion represent their collective slow rotation, an alternative description emerges which can explain the observed C_f distributions, flow dynamics, and the existence of the apparent optimum tandem parameters.

The flow visualization showed that a single plate tended to disrupt the hairpins' collective rotation thus decorrelating the bulge-scale motion in the supposed LEBUs manner. At the same time, perhaps consequentially, it imposed a degree of order on the structures passing beneath it. This resulted in a regularization of production via bursting. Although Corke *et al.* (1982) found that the non-dimensional burst frequency $(u_\tau^2 T/\nu)^{-1}$ was reduced by 17%, Bandyopadhyay (1986) has shown that the average period between bursts (T) was unchanged, so the associated drop in skin friction was probably due to changes in the amplitude and dispersion of burst strengths.

The importance of the length of the plate and particularly the significant improvement in performance when l exceeded δ_m could be connected with the fact that the hairpins in an approaching bulge were moving up through the layer. Consequently one might expect that a plate length greater than half the typical bulge length of approximately $2\delta_m$ would be needed to ensure that a sufficient proportion interacted directly with the plate to disrupt their collective motion.

Preliminary hot-wire measurements (see Savill 1984, 1986) behind a single 3 in. plate have indicated that there was a sharp reduction in u' fluctuations at low wavenumbers associated with the suppression not only of the bulge-scale motions, but also the very large-scale (greater than δ) longitudinal motions which contribute to the inactive motion, presumably as a consequence of the imposed two-dimensional wake. The spectra confirmed that this process was indeed aided by the promotion of an energy cascade to the small-scale eddies introduced into the layer via the wake of the plate. However, it appears that this wake performed two other important functions. First it was seen to act as a shield, preventing incursions of high-speed potential fluid, and blocking the interaction between turbulent fluctuations in the outer part of the layer and the near-wall region. Such an effect has been anticipated by Falco (1983) and is supported by the numerical simulations of Kinney *et al.* (1984). Secondly, as the contrarotating vortices forming the bottom half of the wake approached the wall they tended to cancel the mean flow vorticity and induced a more vertical uplift of newly formed hairpin vortex loops away from the top of the sublayer. The observed reduction in u' intensity at moderate wavenumbers must

surely be related to the decrease in the mean velocity gradient caused by the imposition of the wake defect, to the regularization of turbulence production, and also to the fact that the uplifted hairpins, inclined at angles greater than the maximum straining angle of 45°, would be less efficient at extracting energy from the mean flow, leading to reductions in $-\overline{uv}$ and τ_w also.

All the skin-friction measurements presented in figures 4–7 pointed to a localized influence which spread across the layer from the device to the wall, and the flow visualization indicated that this was connected with the passage of the lower set of wake vortices. The observation that the maximum local skin-friction reduction always occurred at the point where these vortices reached the sublayer and then recovery began after they had been suppressed by the wall suggests that their interaction with the eddy structure in this region was a particularly important mechanism for the reduction of skin friction. If so this would explain why the height of the plate was important because, together with the flow velocity, it determined how quickly the wake vortices reached the wall. Both the maximum local reduction in skin friction and the subsequent variation of C_f seemed to depend on their strength at this stage. Furthermore the hot-wire data indicated that the scale of the wake vortices decreased with increasing U_0, which would explain why the devices then had to be moved closer to the wall to produce the same results. By comparison, it was because the cylinder generated a large-scale street that it had to be placed higher in the boundary layer than the plates in order to produce the maximum C_f reduction at a given distance downstream. When mounted at the same height as the plates its vortices reached the wall sooner, but this rapid growth occurred at the expense of greater mixing so the wake lost its identity sooner and one would expect to see the earlier peak reduction followed by a more rapid recovery, producing a smaller overall C_f reduction, which was observed.

The reduction in entrainment could be attributed initially to the shearing of the hairpin tops towards the stream direction which would reduce their entraining efficiency, and this would also account for the flattening of the interface immediately behind the device. The suppression of the bulge-scale motion, persistent blocking action of the wake and the spreading of the top set of wake vortices to form the interface ensured that this remained relatively flattened further downstream.

All the wakes were enhanced to some extent by the presence of boundary-layer fluctuations at their origin, but there was no evidence of, or indeed need for, any vortex unwinding mechanism. However, following the numerical simulations of Acton & Dhanak (1984); Dowling (1985) it seems possible that the approaching hairpin tops may act in a similar way to enhance the initial strength of the opposite-sign lower set of wake vortices thus counteracting to some extent the weakening influence of the mean shear.

It is also unlikely that the proposed energy transfer mechanism could play a role in the C_f reduction. It would now seem that there are many similarities between manipulated flows and wake/boundary layer interactions of the type studied by Savill & Zhou (1983); Zhou & Squire (1985) where the wake is initiated outside the layer. In the latter case there may on occasion be a significant area over which the shear stress opposes the mean velocity gradient due to countergradient transport driven by large-scale eddies; the so-called negative production region. However, even then it is very rare for a true reverse transfer of energy to occur for the reasons discussed by Hinze (1970). The negative production region is virtually non-existent in the case of a flat-plate wake merging with a boundary layer (Zhou & Squire 1985),

and hot-wire data indicate that it is very small, and restricted to the region immediately behind the obstacle, when either a cylinder (Tsiolakis, Krause & Muller 1983) or a flat plate (Savill 1984) is mounted within the boundary layer.

If the wake plays such a dominant role in the skin-friction reduction it is easy to explain why the tandem arrangement represented such an improvement on a single plate of the same total length, despite the extra 32% drag penalty, because two vortex-street wakes were then generated. Not only should the shielding have been more effective, but two sets of uplifting/contrarotating vortices were introduced into the layer rather than one, and furthermore the second set were amplified owing to the presence of the first. The growth of the second set not only displaced the first towards the wall, hastening the initial skin friction reduction, but their successive interaction with the near-wall structure was apparently responsible for the delayed peak reduction and the extension of the low-C_f region further downstream.

The reported optimum tandem spacing of $s \approx 12\delta$ may be related to the maximum distance over which the first street remained essentially fully coherent, since the degree of amplification of the second street seemed to depend on this. However this also suggests that the gap, g, between the trailing edge of the first plate and the leading edge of the second was a more relevant parameter than s, the spacing between their centres. This would be approximately 8–9δ for typical tandem plates with $s \approx 12\delta$. In fact we observed that the greatest amplification occurred not for this separation, but rather when g was reduced to less than δ so that the instability formed behind the first plate impinged directly onto the leading edge of the second, and this arrangement might therefore offer the possibility of improvements in performance above that for the wider spacing. Indeed Bertelrud *et al.* (1982) obtained their only net reduction with $g = 0.9\delta$ while the results of both Sandborn (1981) and Veuve & Truong (1984) indicate improvements when g was reduced from 1.5δ to 0.5δ.

It would seem then, that at least for our relatively thick devices, a direct interaction between the introduced wake vortices and the near-wall boundary-layer structure provides the primary mechanism for reducing the skin friction, because this would explain the shape of the C_f distributions behind all the devices tested and the optimum values of h and s (or g). The other 'active' mechanisms – the disruption of the bulge-scale motion by the plate, the blocking action of the wake, and the suppression of very low wavenumber longitudinal vortices – apparently only contributed a smaller part of the C_f reduction in the flows studied and so may be regarded as secondary. It was therefore the introduction of new structures into the flow that was most important in these cases, not the destruction or suppression of existing ones. The acronym LEBU is thus misleading and of the various alternative proposals – ribbons, RIOL (ribbons in outer layer), OLD (outer-layer devices), moderators, blades etc. – we prefer the original IIT proposal of manipulators, although the term manipulation is now being used in the wider sense of applying any drag-reduction technique to a flow.

It is possible that the influence of the wake vortices will be much weaker with thinner plates or low-drag aerofoil sections, and this might partly account for the poorer performance reported in some cases for $t < 0.1$ mm, although the vibration of tensioned elements is then a problem which has been shown by Bertelrud *et al.* (1982) to ruin the effect. However as long as an inflexional mean velocity profile is established there is no reason to expect this will be so. We found essentially the same performance when reducing the thickness of our devices from 1.2 to 0.56 mm. From the comparison with other data presented in figures 7, 8 and 9 it appears that there

is little reduction in the efficiency of these devices when t is further reduced to 0.1 mm, and this would seem to be the optimum thickness for flat plates since the device drag is then reduced to just laminar skin friction, maximizing the net reduction. The shapes of the C_f distributions obtained with such net-reduction devices are remarkably-similar to those found behind much thicker plates, which suggests that the skin friction reduction is still due to the same mechanics providing a similar balance of contributions.

In other situations the relative importance of the different mechanisms may be changed. Thus in the presence of free-stream turbulence the blocking influence of the wake could be particularly important because this might prevent any direct influence of the external fluctuations on the wall region leaving only the 'interaction-at-a-distance' effects described by Gartshore, Durbin & Hunt (1983). One might thus find relatively larger drag reductions in that case since the expected increase in C_f due to the free-stream turbulence would be suppressed. Such an effect would be important in any application to internal flows, but most manipulator research to date has been aimed at external applications.

In contrast, if the normally weak bulge-scale motion were artificially amplified the ability of the manipulator plates to disrupt or suppress such motions as a result of the imposed boundary condition would become more significant. This could explain why Hefner *et al.* (1979) were unable to reproduce the larger skin friction and net reductions obtained by Corke *et al.* (1982) because they found that the particular type of sandpaper trip used in the latter experiment produced more large-scale structure and intermittency than existed in other low-Re_θ boundary-layer flows. At the same time one would not expect such enhanced, large-scale, 'relics of transition' to reappear following manipulation.

5. Conclusions

The interaction between flat-plate turbulence manipulators and the hairpin eddy structure of the boundary layer has been examined and it has been shown that the skin-friction reduction behind such devices is due to several 'active' mechanisms as well as the 'passive' effect of the imposed momentum deficit. Of these it appears that an interaction between the introduced wake vortices, of opposite sign to the mean vorticity, and the near-wall flow may play the dominant role. For a single plate the height and flow velocity together determine the rate at which these wake vortices reach the sublayer, their strength at this stage, and hence the C_f distribution. In order to obtain the maximum integrated skin-friction reduction the optimum value of h is approximately 0.75 at the Re_θ of the current experiments, but there is an indication that this should be reduced as Re_θ, U_0 increase, simultaneously taking advantage of the reduced device drag closer to the wall. The length of the plate controls the effectiveness of the large-scale suppression and should be greater than δ_m to take advantage of a step up in performance at that level. With a tandem configuration it appears that the plate separation influences the rate of growth of the second plate's wake which in turn determines to a large extent the magnitude, shape, and hence integrated area, of the C_f distribution. The gap, g, between the first-plate trailing edge and the second-plate leading edge is probably a more relevant parameter than the separation, s, between their centres and this should be either 8δ–9δ or perhaps 0.5δ–1δ. For net reductions with flat-plate devices it seems essential that t be of order 0.1 mm to ensure that the device drag is reduced to just laminar skin friction.

This work was supported by the SERC through Grant No. 3725 (J.C.M.) and by Rolls-Royce plc under University Research Project No. 239 (A.M.S.). The authors are grateful to Dr R. B. Price of the Advanced Research Laboratory, Rolls-Royce plc, Professor J. E. Ffowcs Williams of the University Engineering Department, and Dr A. A. Townsend of the Cavendish Laboratory for initiating many valuable discussions.

REFERENCES

ACHARYA, M. & ESCUDIER, M. P. 1983 Measurements of the wall shear stress in boundary layer flows. In *Proc. 4th Symp. Turbulent Shear Flows, Karlsruhe*, pp. 277–286. Springer.

ACTON, E. & DHANAK, M. 1984 A model of the interaction between a flow manipulator and an approaching vortex. In *Abstr. EUROMECH 181* (see Bertelrud *et al.* 1984).

ANDERS, J. B. 1986 Large eddy breakup devices as low Reynolds number airfoils. *SAE Tech. Paper* 861769.

ANDERS, J. B., HEFNER, J. N. & BUSHNELL, D. M. 1984 Performance of large-eddy breakup devices at post-transitional Reynolds numbers. *AIAA*-84-0345.

ANDERS, J. B. & WATSON, R. D. 1985 Airfoil Large-eddy breakup devices at post transitional Reynolds numbers. *AIAA*-85-0345.

BANDYOPADHYAY, P. R. 1986 Review – Mean flow in turbulent boundary layers disturbed to alter skin friction. *Trans. ASME* I: *J. Fluids Engng.* **108**, 127–145.

BERTELRUD, A. 1984 Full scale experiments into the use of large-eddy breakup devices for drag reduction on aircraft. In *Improvement of Aerodynamic Performance Through Boundary Layer Control and High Lift Systems.* AGARD Conf. Proc. vol. 365, pp. 5.1–10.

BERTELRUD, A. 1986 Manipulated turbulence structure in flight. In *Advances in Turbulence: Proc. European Turbulence Conf., Lyon*, pp. 524–532. Springer.

BERTELRUD, A., DROUGGE, G. & LANDAHL, M. T. 1984 *Drag Reduction through Boundary Layer Control – A report on EUROMECH 181. FFA TN* 1984–60.

BERTELRUD, A., TRUONG, T. V. & AVELLAN, F. 1982 Drag reduction in turbulent boundary layers using ribbons, *AIAA*-82-1370.

BRADSHAW, P. 1972 Two more wind tunnels driven by aerofoil type centrifugal blowers. *Imperial College Dept. Aero. Rep.* 72–10.

CORKE, T. C., GUEZENNIC, Y. & NAGIB, H. M. 1979 Modification in drag of turbulent boundary layers resulting from manipulation of large-scale structures. *Prog. Astronaut Aeronaut* **72**, 128–143.

CORKE, T. C., NAGIB, H. M. & GUEZENNEC, Y. 1982 A new view of the origin, role and manipulation of large scales in turbulent boundary layers. *NASA CR* 165861.

DOWLING, A. P. 1985 The effect of large-eddy breakup devices on oncoming vorticity. *J. Fluid Mech.* **160**, 447–464.

FALCO, R. E. 1979 Structural aspects of turbulence in boundary layer flows. In *Proc. 6th Symp. on Turbulence in Liquids, Missouri-Rolla* (ed. A. R. Patterson & L. Zakin), pp. 1–16.

FALCO, R. E. 1983 New results, a review and synthesis of the mechanism of turbulence production in boundary layers and its modification. *AIAA*-83-0377.

GARTSHORE, I. S., DURBAN, P. A. & HUNT, J. C. R. 1983 The production of turbulent stress in a shear flow by irrotational fluctuations. *J. Fluid Mech.* **137**, 307–330.

HARITONIDIS, J. H., LANDAHL, M. T. & WIDNALL, S. E. 1985 LEBU devices and turbulent boundary layer structure. In *Abstr. ONR-NSSC-AFOSR-NASA Symp. on Drag Reduction and Boundary Layer Control, Washington, DC.*

HEAD, M. R. & BANDYOPADHYAY, P. R. 1981 New aspects of turbulent boundary-layer structure. *J. Fluid Mech.* **107**, 297–338.

HEFNER, J. N., ANDERS, J. B. & BUSHNELL, D. M. 1983 Alteration of outer flow structures for turbulent drag reduction. *AIAA*-83-0193.

HEFNER, J. N., WEINSTEIN, L. M. & BUSHNELL, D. M. 1979 Large-eddy break-up scheme for turbulent viscous drag reduction. *Prog. Astronaut Aeronaut* **72**, 110–127.

HINZE, J. O. 1970 Turbulent flow regions with shear stress and mean velocity gradient of opposite sign. *Appl. Sci. Res.* **22**, 163–175.

HOERNER, S. F. 1965 *Fluid-dynamic Drag: Practical Information on Aerodynamic Drag and Hydrodynamic Resistance*, 2nd Edn. Published by the author, New Jersey, USA.

KINNEY, R. B., TASLIM, M. E. & MUNG, S. C. 1984 Numerical study of large-eddy breakup and its effect on the drag characteristics of boundary layers. *University of Arizona Dept. Aerosp. & Mech. Eng. Tech. Rep.* NAG-1-141.

LEMAY, J., PROVENCAL, D., GORDEAU, R., NGUYEN, V. D. & DICKINSON, J. 1985 More detailed measurements behind turbulence manipulators including tandem devices using servo-controlled balances. *AIAA*-85-0621.

LOERKE, R. I. & NAGIB, H. M. 1972 Experiments on the management of free stream turbulence. *AGARD Rep.* 598.

LOERKE, R. L. & NAGIB, H. M. 1976 Control of free stream turbulence by means of honeycombs: A balance between suppression and generation *Trans. ASME* I: *J. Fluids Engng* **98**, 342–353.

MUMFORD, J. C. & SAVILL, A. M. 1984 Parametric studies of flat plate, turbulence manipulators including direct drag results and laser flow visualisation. In *Laminar Turbulent Boundary Layers Their Control and Flow Over Compliant and Other Surfaces*, vol. 11, pp. 41–51. Fluids Eng. Div. ASME.

NGUYEN, V. D., DICKINSON, J., JEAN, Y., CHALIFOUR, Y., ANDERSON, J., LEMAY, J., HAEBERLE, D. & LAROSE, G. 1984*a* Some experimental observations of the law of the wall behind large-eddy breakup devices using servo-controlled skin friction balances. *AIAA*-84-0346.

NGUYEN, V. D., DICKINSON, J., LEMAY, J., PROVENCAL, D., JEAN, Y. & CHALIFOUR, Y. 1984*b* The determination of turbulent skin friction behind flat plate turbulence manipulators using servo-controlled balances. In *Proc. 14th ICAS Congr., Toulouse*, pp. 1–6.

NGUYEN, V. D., SAVILL, A. M. & WESTPHAL, R. V. 1987 Direct local skin friction measurements following turbulence manipulation. *AIAA J.* **25**, 498–500.

PERRY, A. E. & CHONG, M. S. 1982 On the mechanism of wall turbulence. *J. Fluid Mech.* **119**, 173–218.

PLESNIAK, M. W. & NAGIB, H. M. 1985 Net drag reduction in turbulent boundary layers resulting from optimised manipulation. *AIAA*-85-0518.

POLL, D. I. A. & WATSON, R. D. 1984 On the relaxation of a turbulent boundary layer after an encounter with a forward facing step. In *Improvement of Aerodynamic Performance Through Boundary Layer Control and High Lift Systems*. AGAR Conf. Proc. vol. 365, pp. 18.1–10.

SANDBORN, V. A. 1981 Control of surface shear stress fluctuations in turbulent boundary layers. *Colorado State University Rep.* CER 80–81 VAS 46.

SAVILL, A. M. 1979 Effects on turbulence of curved or distorting mean flow. Ph.D. thesis, University of Cambridge.

SAVILL, A. M. 1984 The skin friction reduction mechanisms of flat plate, turbulence manipulators. In *Abstr. EUROMECH 181* (see Bertelrud *et al.* 1984).

SAVILL, A. M. 1986 On the manner in which outer layer disturbances affect turbulent boundary layer skin friction. In *Advances in Turbulence: Proc. European Turbulence Conf., Lyon*, pp. 533–545. Springer.

SAVILL, A. M. & ZHOU, M. D. 1983 Wake/boundary layer and wake/wake interactions – Smoke flow visualisation and modelling. In *Proc. 2nd Asian Congr. Fluid Mech. Beijing*, pp. 743–755. China: Science Press.

TAKAGI, S. 1983*a* The structure of turbulent boundary layer controlled by the plates. In *Proc. 15th Turbulence Symp., Tokyo.*

TAKAGI, S. 1983*b* On the mechanism of drag reduction in a turbulent boundary layer using a thin plate. In *Proc. 2nd Asian Congr. Fluid Mech., Beijing*, p. 292. China: Science Press.

TRUONG, T. V., BERTELRUD, A. & VEUVE, M. 1984 Boundary layer development downstream of transverse ribbons. In *Abstr. EUROMECH 181* (see Bertelrud *et al.* 1984).

TSIOLAKIS, E. P., KRAUSE, & E. MULLER, U. R. 1983 Turbulent boundary layer-wake interaction. In *Proc. 4th Symp. Turbulent Shear Flows, Karlsruhe*, pp. 287–298. Springer.

VEUVE, M. & TRUONG, T. V. 1984 Drag reduction in turbulent boundary layers using thin transverse ribbons. In *Abstr. EUROMECH 181* (see Bertelrud *et al.* 1984).

WALLACE, J. M., BALINT, J.-L., MAURIAUX, J.-L. & MOREL, R. 1983 Observations on the nature and mechanism of turbulent boundary layers: A survey and new results. In *Proc. ASCE EMD Speciality Conf., Purdue University*, pp. 1–6.

WESTPHAL, R. V. 1986 Skin friction and Reynolds stress measurements for a turbulent boundary layer following manipulation using flat plates. *AIAA*-86-0283.

WINTER, K. G. 1977 An outline of the techniques available for the measurement of skin friction in turbulent boundary layers. *Prog. Aerospace Sci.* **18**, 1–57.

YAJNIK, K. S. & ACHARYA, M. 1977 Non-equilibrium effects in a turbulent boundary layer due to the destruction of large eddies. In *Structure and Mechanisms of Turbulence*, Lecture Notes in Physics, vol. 76, pp. 249–260. Springer.

ZHOU, M. D. & SQUIRE, L. C. 1985 The interaction of a wake with a boundary layer. *Aeronaut. J.* **89**, 72–81.